

Article

Intensity Evolution of Cosine-Gaussian-Correlated Schell-Model Pulse Scattered by a Medium

Haixia Wang *, Xumin Yan, Xiaotong Feng, Zhiguo Zhao and Liuzhan Pan

College of Physics and Electronic Information and Henan Key Laboratory of Electromagnetic Transformation and Detection, Luoyang Normal University, Luoyang 471934, China; xuminyanlynu@163.com (X.Y.); xiaotongfenglysy@163.com (X.F.); zhiguo.zhao@lynu.edu.cn (Z.Z.); liuzhanpan@lynu.edu.cn (L.P.)

* Correspondence: haixiawang@lynu.edu.cn; Tel.: +86-379-6861-8310

Received: 18 January 2020; Accepted: 2 March 2020; Published: 6 March 2020



Abstract: According to first-order Born approximation, the scattering of a partially coherent pulse with cosine-Gaussian correlation by a medium was studied. On the basis of analytic expression, the changes in intensity evolution of the scattered pulse are discussed. The influences of pulse and medium characteristics on the intensity of the scattered pulse were investigated. The intensities of a Gaussian Schell-model (GSM) pulse and a cosine-Gaussian-correlated Schell-model (CGSM) pulse, both scattered by the same medium, are compared, and their similarities and differences are examined in detail. The effective angular width of the scattered pulse could be modulated by the parameters of the pulse and medium. The obtained results could find potential applications in pulsed beam scattering.

Keywords: coherence optics; scattering; quasihomogeneous media; CGSM pulse; intensity

1. Introduction

Light scattering has received continuous attention from researchers because of its potential applications in some areas, like medical detection and ocean remote sensing. Since pioneering research in 1870, many studies have been carried out in this field, where the optical statistical characteristics of a scattered pulse, such as intensity, polarization, and coherence, were extensively studied [1–4]. The inverse problem, obtaining information on a scatterer through the characteristics of a scattered pulse, was also examined [5,6]. However, most of the above investigations were carried out on the scattering of statistically stationary fields.

The optical pulse is an important part of a broad class of light beams [7]. The basic concepts and representations of partially coherent pulses were established [8,9]. In the discussion of pulsed-beam scattering [10–16], the initial pulse was fully or partially coherent, and the complex degree of coherence of the majority of these partially coherent pulses is a conventional Gaussian Schell-mode function [17]. In recent years, a large number of partially coherent sources with other types of Schell-mode coherence were proposed, e.g., nonuniform-correlation [18], multi-Gaussian Schell-model [19,20], Laguerre-Gaussian and Hermite-Gaussian Schell-model [21], and sinc-correlation sources [22]. Some experiments related to the realization of these pulses have also been made [23,24].

We studied the scattering of a cosine-Gaussian-correlated Schell-model (CGSM) pulse on a quasihomogeneous medium, and investigated the intensity evolution of the scattered pulse within the accuracy of first-order Born approximation. We pay more attention to examining the intensity variation of the scattered pulse with order-parameter n , duration, the temporal-coherence length of the initial pulse, and the radius and correlation length of the medium.

2. Theory

The temporal mutual coherence function for a CGSM pulse has the following form [19]:

$$\Gamma(t_1, t_2) = \langle E^*(t_1)E(t_2) \rangle = \Gamma_0 \exp\left[-\frac{t_1^2 + t_2^2}{4T_0^2} - \frac{(t_2 - t_1)^2}{2T_c^2} + i\omega_0(t_1 - t_2)\right] \cos\left(\frac{n\sqrt{2\pi}(t_2 - t_1)}{T_c}\right), \quad (1)$$

where $E(t_1)$ and $E(t_2)$ are the complex analytic signals of pulse realizations at time t_1 and t_2 , respectively; the asterisk is the complex conjugate; Γ_0 is a positive constant; T_0 represents the pulse duration; T_c is the temporal-coherence length denoting the temporal correlation of the pulse; ω_0 describes the carrier frequency of the pulse [25]; n is a constant greater than zero and does not need to be an integer. Obviously, for the case of $n = 0$, a CGSM pulse is simplified to a GSM pulse.

By performing Fourier transform on Equation (1), the cross-spectral density function for a CGSM pulse is given by [11]

$$W(\omega_1, \omega_2) = W_0 \exp\left[-\frac{(\omega_1 - \omega_0)^2 + (\omega_2 - \omega_0)^2}{2\Omega_0^2}\right] \exp\left[-\frac{(\omega_1 - \omega_2)^2}{2\Omega_c^2}\right] \times \exp\left[-\frac{\sqrt{2\pi}nb}{T_c}\right] \cosh[b(\omega_1 + \omega_2 - 2\omega_0)], \quad (2)$$

where

$$W_0 = \frac{\sqrt{2}T_0}{2\pi\Omega_0} \Gamma_0 \quad (3)$$

$$\Omega_0 = \sqrt{\frac{1}{2T_0^2} + \frac{2}{T_c^2}} \quad (4)$$

$$\Omega_c = \frac{\sqrt{2}T_c}{2T_0} \Omega_0 \quad (5)$$

$$b = \frac{n\sqrt{2\pi}}{\Omega_0^2 T_c}, \quad (6)$$

where Ω_0 denotes the spectral width of the CGSM pulse. Ω_c represents the spectral coherence width of the pulse. $\cosh(x)$ is a hyperbolic cosine function.

Suppose a CGSM pulsed beam is incident on a scatterer along the direction described by unit vector \mathbf{s}_0 (Figure 1). The cross-spectral density of a CGSM pulse at two points with position vectors \mathbf{r}_1' and \mathbf{r}_2' can be written as [26]

$$W^{(i)}(\mathbf{r}_1', \mathbf{r}_2', \omega_1, \omega_2) = W_0 \exp\left[-\frac{(\omega_1 - \omega_0)^2 + (\omega_2 - \omega_0)^2}{2\Omega_0^2}\right] \exp\left[-\frac{(\omega_1 - \omega_2)^2}{2\Omega_c^2}\right] \times \exp\left[-\frac{\sqrt{2\pi}nb}{T_c}\right] \cosh[b(\omega_1 + \omega_2 - 2\omega_0)] \exp[i(k_2\mathbf{s}_0 \cdot \mathbf{r}_2' - k_1\mathbf{s}_0 \cdot \mathbf{r}_1')] \quad (7)$$

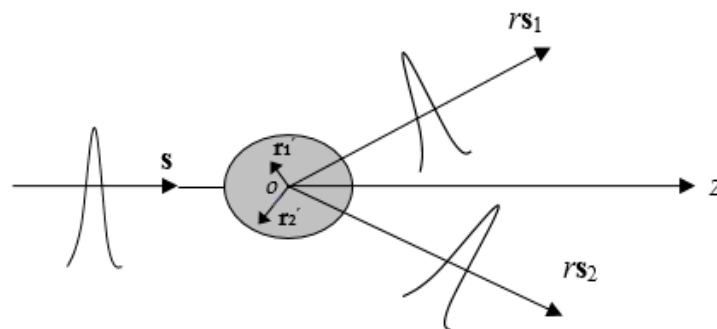


Figure 1. Notation relating to scattering a cosine-Gaussian-correlated Schell-model (CGSM) pulse by a medium.

In the scattering process, the correlation function of the scattering potential is used to describe the scattering properties of a random medium [27]. In [10], it was assumed that the resonance frequency of molecules or atoms in the medium is approximately represented by the carrier frequency of the pulse. Therefore, the correlation function of the scattering potential is expressed as [28,29]

$$C_F(\mathbf{r}'_1, \mathbf{r}'_2, \omega) = \langle F^*(\mathbf{r}'_1, \omega)F(\mathbf{r}'_2, \omega) \rangle_m = \langle F^*(\mathbf{r}'_1, \omega_0)F(\mathbf{r}'_2, \omega_0) \rangle_m = C_F(\mathbf{r}'_1, \mathbf{r}'_2, \omega_0), \tag{8}$$

where $F(\mathbf{r}', \omega)$ is defined as the scattering potential of the medium, and $\langle \cdot \rangle$ denotes averaging over the ensemble of a random medium [30].

According to the first-order Born approximation, we obtained the formula for the cross-spectral density function of the scattered pulse [31,32]:

$$W^{(s)}(r\mathbf{s}_1, r\mathbf{s}_2, \omega_1, \omega_2) = W_0 \exp\left[-\frac{(\omega_1-\omega_0)^2+(\omega_2-\omega_0)^2}{2\Omega_0^2} - \frac{(\omega_1-\omega_2)^2}{2\Omega_c^2}\right] \frac{\exp[i\mathbf{r}(k_2-k_1)]}{r^2} \times \exp\left[-\frac{\sqrt{2\pi}nb}{T_c}\right] \cosh[b(\omega_1 + \omega_2 - 2\omega_0)] \int_D \int_D C_F(\mathbf{r}'_1, \mathbf{r}'_2, \omega_0) \exp[-i(\mathbf{K}_1 \cdot \mathbf{r}'_1 + \mathbf{K}_2 \cdot \mathbf{r}'_2)] d^3r'_1 d^3r'_2, \tag{9}$$

where $r\mathbf{s}_1$ and $r\mathbf{s}_2$ are the position vectors of two observation points (\mathbf{s}_1 and \mathbf{s}_2 are unit vectors). $\mathbf{K}_1 = -k_1(\mathbf{s}_1 - \mathbf{s}_0)$ and $\mathbf{K}_2 = k_2(\mathbf{s}_2 - \mathbf{s}_0)$ are the momentum-transfer vectors. D is the domain that the medium occupies.

A quasihomogeneous medium was considered in this paper of which the correlation function of the scattering potential is given by [1,29,33]

$$C_F(\mathbf{r}'_1, \mathbf{r}'_2, \omega_0) = C_0 \exp\left[-\frac{|\mathbf{r}'_1 + \mathbf{r}'_2|^2}{8\sigma_R^2}\right] \exp\left[-\frac{|\mathbf{r}'_1 - \mathbf{r}'_2|^2}{2\sigma_r^2}\right], \tag{10}$$

where C_0 is a positive constant, σ_R is the effective radius of the medium, and σ_r is the correlation length of the media, which must satisfy inequality $\sigma_R \geq \sigma_r$.

When we substitute from Equation (10) into Equation (9), we can obtain the cross-spectral density of a pulse scattered by a medium [34]:

$$W^{(s)}(r\mathbf{s}_1, r\mathbf{s}_2, \omega_1, \omega_2) = W_0 C_0 (2\pi\sigma_R\sigma_r)^3 \exp\left[-\frac{(\omega_1-\omega_0)^2+(\omega_2-\omega_0)^2}{2\Omega_0^2} - \frac{(\omega_1-\omega_2)^2}{2\Omega_c^2}\right] \exp\left[-\frac{\sqrt{2\pi}nb}{T_c}\right] \times \cosh[b(\omega_1 + \omega_2 - 2\omega_0)] \frac{\exp[i\mathbf{r}(k_2-k_1)]}{r^2} \exp\left[-\frac{1}{2}\sigma_R^2(\mathbf{K}_1 + \mathbf{K}_2)^2 - \frac{1}{8}\sigma_r^2(\mathbf{K}_1 - \mathbf{K}_2)^2\right]. \tag{11}$$

By using the inverse Fourier transform of Equation (11), the mutual-coherence function of the scattered pulse is expressed by the following formula:

$$\Gamma^{(s)}(r\mathbf{s}, r\mathbf{s}, t_1, t_2) = \frac{W_0 C_0 (2\pi\sigma_R\sigma_r)^3}{r^2 \sqrt{2(T_0^2+m+a)} \left[1+(m-a)\frac{T_c^2+4T_0^2}{T_c^2 T_0^2}\right]} \exp\left[-\frac{(t_1-\frac{t}{c})^2+(t_2-\frac{t}{c})^2}{4(T_0^2+m+a)}\right] \times \exp\left[-\frac{(\frac{2T_0^2}{T_c^2}+a\frac{T_c^2+4T_0^2}{T_c^2 T_0^2})(t_1-t_2)^2}{4(T_0^2+m+a)\left[1+(m-a)\frac{T_c^2+4T_0^2}{T_c^2 T_0^2}\right]}\right] \exp\left[\frac{i\omega_0(t_1-t_2)}{1+(m-a)\frac{T_c^2+4T_0^2}{T_c^2 T_0^2}}\right] \times \exp\left[-\frac{2\omega_0^2(m-a)-b^2\frac{T_c^2+4T_0^2}{2T_c^2 T_0^2}}{1+(m-a)\frac{T_c^2+4T_0^2}{T_c^2 T_0^2}} - \frac{\sqrt{2\pi}nb}{T_c}\right] \cosh\left[\frac{b[2\omega_0(m-a)-\frac{1}{2}(t_1-t_2)]}{\frac{T_c^2 T_0^2}{T_c^2+4T_0^2}+m-a}\right], \tag{12}$$

where

$$m = \frac{\sin^2 \frac{\theta}{2} (4\sigma_R^2 + \sigma_r^2)}{2c^2} \tag{13}$$

$$a = \frac{\sin^2 \frac{\theta}{2} (4\sigma_R^2 - \sigma_r^2)}{2c^2}. \tag{14}$$

With the help of unified theory [35,36], where spectral density, spectral degree of coherence, and spectral degree of polarization can be treated in the same manner, the intensity of the scattered pulse has the following form.

$$I^{(s)}(rs, t) = \frac{W_0 C_0 (2\pi\sigma_R\sigma_r)^3}{r^2 \sqrt{2(T_0^2+m+a) \left[1+(m-a) \frac{T_c^2+4T_0^2}{T_c^2 T_0^2} \right]}} \exp\left[-\frac{(t-\frac{r}{c})^2}{2(T_0^2+m+a)}\right] \times \exp\left[-\frac{2\omega_0^2(m-a)-b^2 \frac{T_c^2+4T_0^2}{2T_c^2 T_0^2}}{1+(m-a) \frac{T_c^2+4T_0^2}{T_c^2 T_0^2}} - \frac{\sqrt{2\pi}nb}{T_c}\right] \cosh\left[\frac{2b\omega_0(m-a)}{\frac{T_c^2 T_0^2}{T_c^2+4T_0^2} + m-a}\right] \tag{15}$$

3. Intensity Properties of CGSM Pulse Scattered by a Medium

On the basis of Equation (15), the intensity involution of a CGSM pulse scattered by a random medium can be studied as follows. Figure 2 shows changes in the normalized intensity of the scattered pulse with the scattering angle for four different values of parameter n . In the following numerical calculations, unless specified otherwise, parameters were chosen as: $T_0 = T_c = 5$ fs, $\lambda_0 = 800$ nm, $\sigma_R = 10 \lambda_0$, $\sigma_r = \lambda_0$, and $t = r/c$. Figure 2 shows that the intensity properties of the scattered CGSM pulse were closely related to parameter n . For a GSM pulse, the intensity distribution of the scattered pulse has Gaussian distribution. With an increase of parameter n , the effective angular width of the scattered pulse decreases. Here, the effective angular width of the scattered pulse is defined as the $1/e$ point of the normalized intensity of the scattered pulse [37].

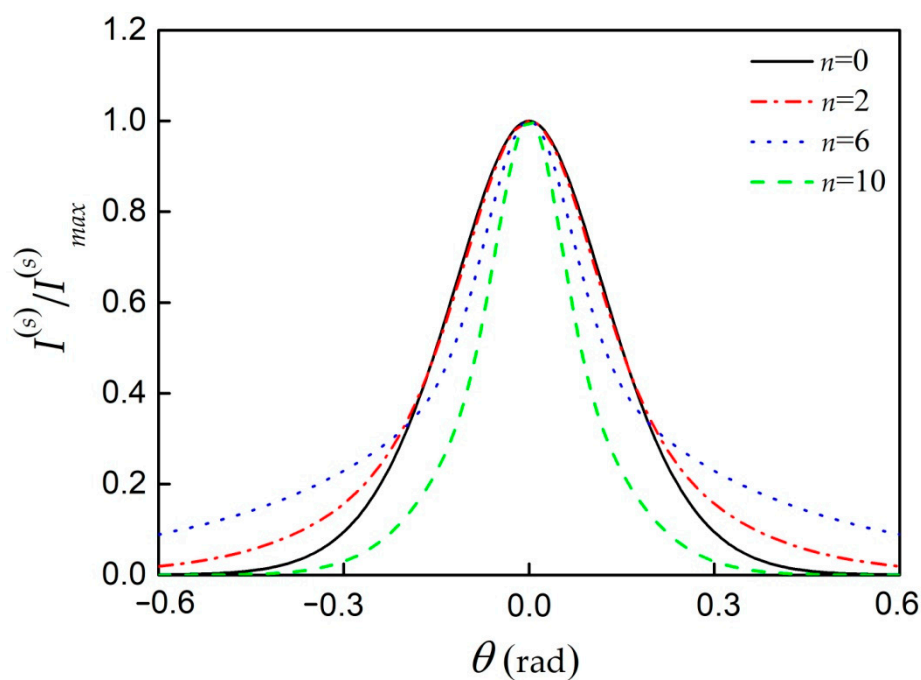


Figure 2. Normalized intensity of scattered pulse as function of scattering angle θ for four different values of parameter n .

Figure 3a illustrates the variations of the normalized intensity of the scattered pulse with scattering angle θ , $n = 2$. In order to display the impact of initial pulse duration T_0 on the intensity of the scattered pulse, Figure 3b gives the changes of the effective angular width of the scattered pulse with initial pulse duration T_0 . It is clear from Figure 3a that the effective angular width of the scattered pulse increased when the initial pulse duration T_0 increased. Furthermore, Figure 3b shows that, for small values of parameter n , the effective angular width of the scattered pulse varied rapidly with initial pulse duration T_0 ; however, it changed slowly for large values of parameter n .

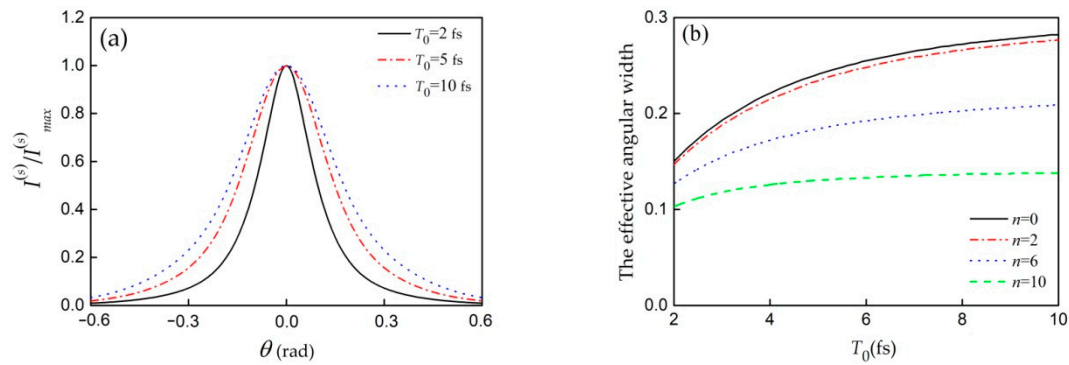


Figure 3. (a) Normalized intensity of scattered pulse against scattering angle θ for different initial pulse duration T_0 . (b) Effective angular width of scattered pulse against initial pulse duration T_0 .

Figure 4 shows (a) the behavior of the normalized intensity of the scattered pulse as a function of scattering angle θ , and (b) the effective angular width of the scattered pulse against temporal-coherence length T_c of the initial pulse. The effective angular width of the scattered pulse increased with increasing temporal-coherence length T_c of the initial pulse. However, the effective angular width of the scattered pulse changed rapidly with temporal-coherence length T_c for large values of parameter n . Especially with an increase of temporal-coherence length T_c of the initial pulse, the effective angular width of the scattered pulse remained nearly unchanged for the case of $n = 0$, and it converged to a constant 0.241 for the case of $n = 0, 2, 6, 10$. The reason for this phenomenon is as follows.

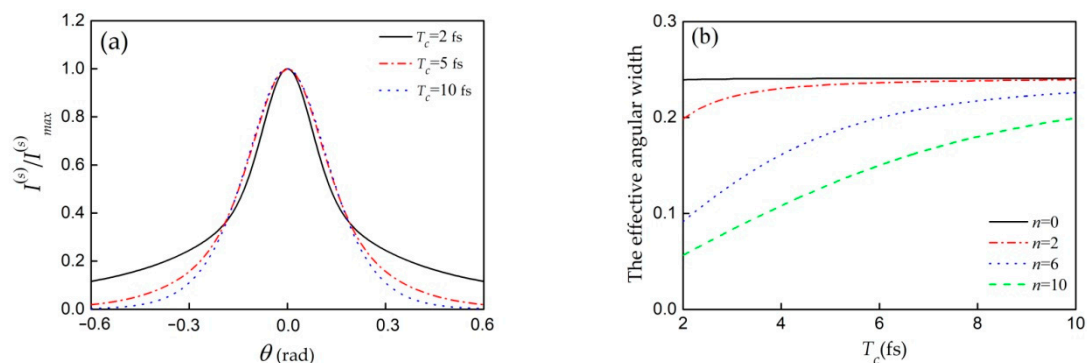


Figure 4. (a) Normalized intensity of scattered pulse against scattering angle θ ; (b) effective angular width of scattered pulse against temporal-coherence length T_c of initial pulse.

When temporal-coherence length T_c of the initial pulse is infinite, the intensity of the scattered pulse takes the following form:

$$I^{(s)}(rs, t) = \frac{W_0 C_0 T_0 (2\pi\sigma_R\sigma_r)^3}{r^2 \sqrt{2(T_0^2 + m + a)} [T_0^2 + (m - a)]} \exp\left[-\frac{(t - \frac{r}{c})^2}{2(T_0^2 + m + a)}\right] \exp\left[-\frac{2\omega_0^2 T_0^2 (m - a)}{T_0^2 + (m - a)}\right], \quad (16)$$

which is independent of temporal-coherence length T_c of the initial pulse and parameter n . Therefore, the effective angular width of the scattered pulse converged to a constant when temporal-coherence length T_c of the initial pulse increased for different n parameters.

Figure 5 illustrates the influence of effective radius σ_R of the medium on the normalized intensity of the scattered pulse. As shown in Figure 5, the effective angular width of the scattered pulse increased as effective radius σ_R of the medium decreased. For large values of parameter n , effective radius σ_R of the medium had little impact on the effective angular width of the scattered pulse.

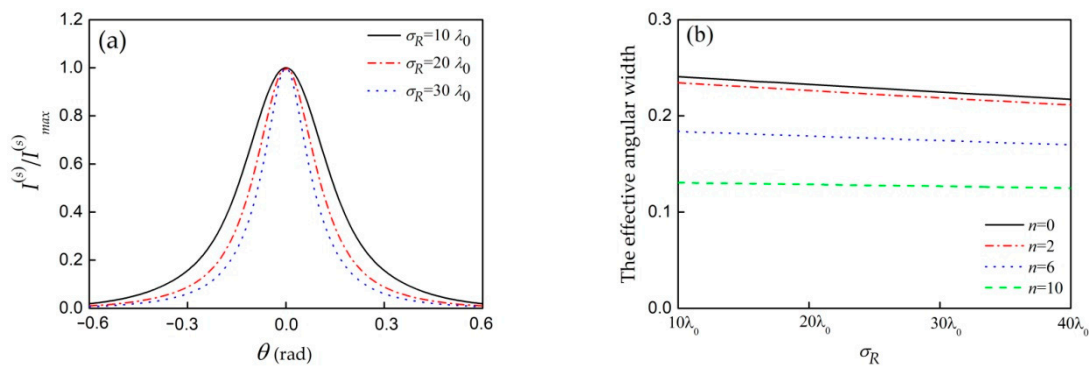


Figure 5. (a) Normalized intensity of scattered pulse against scattering angle θ for three different values of effective radius σ_R of medium. (b) Effective angular width of scattered pulse against effective radius σ_R of medium.

Figure 6 displays the effect of correlation length σ_r of the medium on the normalized intensity of the scattered pulse. The effective angular width of the scattered pulse decreased with increasing correlation length σ_r of the medium. In comparison with effective radius σ_R , the correlation length σ_r of the medium resulted in a more rapid change in the effective angular width of the scattered pulse.

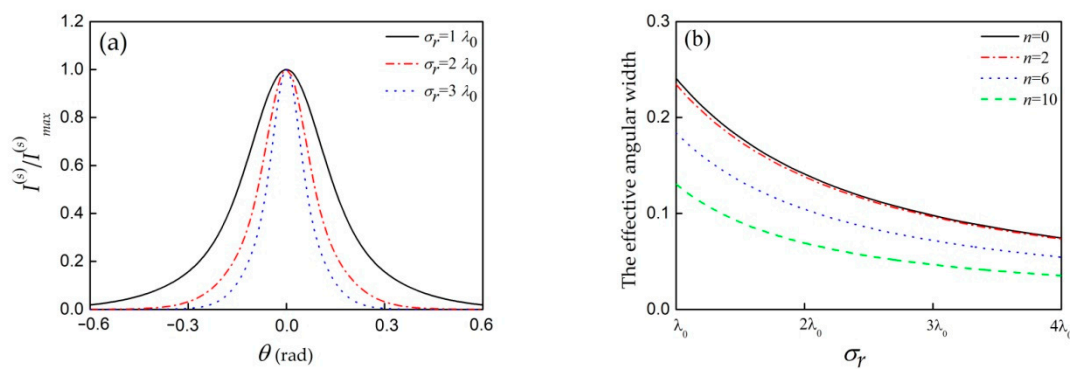


Figure 6. (a) Normalized intensity of scattered pulse against scattering angle θ for three different values of correlation length σ_r of medium. (b) Effective angular width of scattered pulse against correlation length σ_r of medium.

4. Conclusions

In summary, we investigated the intensity evolution of a CGSM pulse scattered by a quasihomogeneous medium on the basis of the scattering theory of nonstationary fields. We derived the closed-form formula for the intensity of the scattered pulse in the time domain. We found that the effective angular width of the scattered pulse can be modulated by the pulse and medium parameters. It increased when the pulse parameters increased or the medium parameters decreased. When variations in the correlation length of the medium and the effective radius of the medium were the same, the former resulted in a more rapid change in the effective angular width of the scattered pulse. In addition, the intensity properties of the scattered CGSM pulse were closely related to the n parameter. Variations of the effective angular width of the scattered pulse induced by parameter n were analyzed in detail. For large values of parameter n , the effective angular width of the scattered pulse changed slowly with the initial pulse duration, and sharply with the temporal-coherence length of the pulse. These results might find uses in practical applications of pulsed-beam scattering.

Author Contributions: Data curation, writing—original draft, and methodology, H.W.; writing—review and editing, X.Y. and X.F.; formal analysis, Z.Z.; project administration, Z.Z. and L.P.; funding acquisition, L.P. All authors have read and agreed to the published version of the manuscript.

Funding: This research was funded by the National Natural Science Foundation of China (grant number 61675094) and the Foundation of Henan Educational Committee (2016GGJS-116).

Conflicts of Interest: The authors declare no conflict of interest.

References

1. Wolf, E.; Foley, J.T. Scattering of electromagnetic fields of any state of coherence from space-time fluctuations. *Phys. Rev. A* **1989**, *40*, 579–587. [[CrossRef](#)]
2. Wu, H.; Pan, X.N.; Zhu, Z.H.; Ji, X.L.; Wang, T. Reciprocity relations of an electromagnetic light wave on scattering from a quasi-homogeneous anisotropic media. *Opt. Express* **2017**, *25*, 11297–11305. [[CrossRef](#)]
3. Wang, F.; Chen, Y.H.; Liu, X.L.; Cai, Y.J.; Ponomarenko, S.A. Self-reconstruction of partially coherent light beams scattered by opaque obstacles. *Opt. Express* **2016**, *24*, 23735–23746. [[CrossRef](#)]
4. Jung, J.H.; Kim, J.; Seo, M.K.; Park, Y.K. Measurements of polarization-dependent angle-resolved light scattering from individual microscopic samples using Fourier transform light scattering. *Opt. Express* **2018**, *26*, 7701–7710. [[CrossRef](#)]
5. Zhao, D.M.; Korotkova, O.; Wolf, E. Application of correlation-induced spectral changes to inverse scattering. *Opt. Lett.* **2007**, *32*, 3483–3485. [[CrossRef](#)]
6. Lahiri, M.; Wolf, E.; Fischer, D.G.; Shirai, T. Determination of correlation functions of scattering potentials of stochastic media from scattering experiments. *Phys. Rev. Lett.* **2009**, *102*, 123901. [[CrossRef](#)]
7. Agrawal, G.P. *Nonlinear Fiber Optics*, 4th ed.; Academic: New York, NY, USA, 2007.
8. Pääkkönen, P.; Turunen, J.; Vahimaa, P.; Friberg, A.T.; Wyrowski, F. Partially coherent Gaussian pulses. *Opt. Commun.* **2002**, *204*, 53–58.
9. Lajunen, H.; Vahimaa, P.; Tervo, J. Theory of spatially and spectrally partially coherent pulses. *J. Opt. Soc. Am. A* **2005**, *22*, 1536–1545. [[CrossRef](#)]
10. Ding, C.L.; Cai, Y.J.; Korotkova, O.; Zhang, Y.T.; Pan, L.Z. Scattering-induced changes in the temporal coherence length and the initial pulse duration of a partially coherent plane-wave pulse. *Opt. Lett.* **2011**, *36*, 517–519. [[CrossRef](#)]
11. Wang, H.X.; Ding, C.L.; Ma, B.H.; Zhao, C.H.; Pan, L.Z. The intensity properties of a multi-Gaussian Schell-model pulse scattering from a sphere with semisoft boundaries. *Opt. Quant. Electron* **2016**, *48*, 1–12. [[CrossRef](#)]
12. Wang, H.X.; Ding, C.L.; Ma, B.H.; Zhao, C.H.; Pan, L.Z. Statistical properties of a stochastic electromagnetic pulse scattering by a quasi-homogeneous random medium. *Opt. Quant. Electron* **2015**, *47*, 3365–3380. [[CrossRef](#)]
13. Ding, C.L.; Cai, Y.J.; Zhang, Y.T.; Pan, L.Z. Scattering of a partially coherent plane-wave pulse on a deterministic sphere. *Phys. Lett. A* **2012**, *376*, 2697–2702. [[CrossRef](#)]
14. Devaux, F.; Lantz, E. 3D-PSTD simulation and polarization analysis of a light pulse transmitted through a scattering media. *Opt. Express* **2013**, *21*, 24969–24984. [[CrossRef](#)]
15. Mounaix, M.; Defienne, H.; Gigan, S. Deterministic light focusing in space and time through multiple scattering media with a time-resolved transmission matrix approach. *Phys. Rev. A* **2016**, *94*, 041802. [[CrossRef](#)]
16. Eggert, J.; Bourdon, B.; Nolte, S.; Rischmueller, J.; Imlau, M. Chirp control of femtosecond-pulse scattering from drag-reducing surface-relief gratings. *Photon. Res.* **2018**, *6*, 542–548. [[CrossRef](#)]
17. Wang, F.; Cai, Y.J.; Lin, Q. Experimental observation of truncated fractional Fourier transform for a partially coherent Gaussian Schell-model beam. *J. Opt. Soc. Am. A* **2008**, *25*, 2001–2010. [[CrossRef](#)]
18. Lajunen, H.; Saastamoinen, T. Non-uniformly correlated partially coherent pulses. *Opt. Express* **2013**, *21*, 190–195. [[CrossRef](#)]
19. Ding, C.L.; Korotkova, O.; Zhang, Y.T.; Pan, L.Z. Cosine-Gaussian correlated Schell-model pulsed beams. *Opt. Express* **2014**, *22*, 931–942. [[CrossRef](#)]
20. Yao, M.; Korotkova, O.; Ding, C.L.; Pan, L.Z. Position modulation with random pulses. *Opt. Express* **2014**, *22*, 16197–16206. [[CrossRef](#)]
21. Ding, C.L.; Koivurova, M.; Turunen, J.; Pan, L.Z. Temporal self-splitting of optical pulses. *Phys. Rev. A* **2018**, *97*, 053838. [[CrossRef](#)]

22. Zhao, Z.G.; Ding, C.L.; Zhang, Y.T.; Pan, L.Z. Spatial-Temporal Self-Focusing of Partially Coherent Pulsed Beams in Dispersive Medium. *Appl. Sci.* **2019**, *9*, 3616. [[CrossRef](#)]
23. Torres-Company, V.; Mínguez-Vega, G.; Lancis, J.; Friberg, A.T. Controllable generation of partially coherent light pulses with direct space-to-time pulse shaper. *Opt. Lett.* **2007**, *32*, 1608–1610. [[CrossRef](#)] [[PubMed](#)]
24. Turunen, J. Low-coherence laser beams. In *Laser Beam Propagation: Generation and Propagation of Customized Light*; Forbes, A., Ed.; CRC Press: Boca Raton, FL, USA, 2014.
25. Ding, C.L.; Pan, L.Z.; Lü, B.D. Phase singularities and spectral changes of spectrally partially coherent higher-order Bessel-Gauss pulsed beams. *J. Opt. Soc. Am. A* **2009**, *26*, 2654–2661. [[CrossRef](#)] [[PubMed](#)]
26. Wang, T.; Zhao, D.M. Scattering of scalar light wave from a Gaussian–Schell model medium. *Chin. Phys. B* **2010**, *19*, 084201.
27. Ding, C.L.; Cai, Y.J.; Zhang, Y.T.; Pan, L.Z. Scattering-induced changes in the degree of polarization of a stochastic electromagnetic plane-wave pulse. *J. Opt. Soc. Am. A* **2012**, *29*, 1078–1090. [[CrossRef](#)] [[PubMed](#)]
28. Wolf, E. *Principles of Optics*; Cambridge University Press: Cambridge, UK, 2007.
29. Foley, J.T.; Wolf, E. Frequency shifts of spectral lines generated by scattering from space-time fluctuations. *Phys. Rev. A* **1989**, *40*, 588–598. [[CrossRef](#)] [[PubMed](#)]
30. Wang, H.; Li, X.Y. Propagation of partially coherent controllable dark hollow beams with various symmetries in turbulent atmosphere. *Opt. Laser Eng.* **2010**, *48*, 48–57. [[CrossRef](#)]
31. Zhang, Y.Y.; Zhao, D.M. The coherence and polarization properties of electromagnetic rectangular Gaussian Schell-model sources scattered by a deterministic medium. *J. Opt.* **2014**, *16*, 125709. [[CrossRef](#)]
32. Wolf, E. *Introduction to the Theory of Coherence and Polarization of Light*, 1st ed.; Cambridge University Press: Cambridge, UK, 2007.
33. Zhang, Y.Y.; Zhao, D.M. Scattering of Hermite–Gaussian beams on Gaussian Schell-model random media. *Opt. Commun.* **2013**, *300*, 38–44. [[CrossRef](#)]
34. Mao, H.D.; Chen, Y.H.; Liang, C.H.; Chen, L.F.; Cai, Y.J.; Ponomarenko, S.A. Self-steering partially coherent vector beams. *Opt. Express* **2019**, *27*, 14353–14368. [[CrossRef](#)]
35. Wolf, E. Unified theory of coherence and polarization of random electromagnetic beams. *Phys. Lett. A* **2003**, *312*, 263–267. [[CrossRef](#)]
36. Zhu, Y.B.; Zhao, D.M. Propagation of a random electromagnetic beam through a misaligned optical system in turbulent atmosphere. *J. Opt. Soc. Am. A* **2008**, *25*, 2408–2414. [[CrossRef](#)]
37. Visser, T.D. *Optical Coherence*; Wiley Online Library: Hoboken, NJ, USA, 2016.



© 2020 by the authors. Licensee MDPI, Basel, Switzerland. This article is an open access article distributed under the terms and conditions of the Creative Commons Attribution (CC BY) license (<http://creativecommons.org/licenses/by/4.0/>).